Designer Protein-Based Performance Materials

Manoj Kumar,* Karl J. Sanford, William P. Cuevas, Mai Du, Katharine D. Collier, and Nicole Chow

Genencor International, a Danisco Company, 925 Page Mill Road, Palo Alto, California 94304

Received May 12, 2006; Revised Manuscript Received June 30, 2006

Repeat sequence protein polymer (RSPP) technology provides a platform to design and make protein-based performance polymers and represents the best nature has to offer. We report here that the RSPP platform is a novel approach to produce functional protein polymers that have both biomechanical and biofunctional blocks built into one molecule by design, using peptide motifs. We have shown that protein-based designer biopolymers can be made using recombinant DNA technology and fermentation and offer the ability to screen for desired properties utilizing the tremendous potential diversity of amino acid combinations. The technology also allows for large-scale manufacturing with a favorable fermentative cost-structure to deliver commercially viable performance polymers. Using three diverse examples with antimicrobial, textile targeting, and UV-protective agent, we have introduced functional attributes into structural protein polymers and shown, for example, that the functionalized RSPPs have possible applications in biodefense, industrial biotechnology, and personal care areas. This new class of biobased materials will simulate natural biomaterials that can be modified for desired function and have many advantages over conventional petroleum-based polymers.

1. Introduction

The concept of using a library of monomers, for example, peptide motifs, and having methods to precisely order them using bottom-up strategies to develop performance protein polymers, is a long sought after objective of material scientists.[1] With the development of protein engineering, protein expression, nano(bio)technology, and the ability to use 20 plus amino acids in designing and producing genetically engineered functional protein polymers that target specific or multifunctional property space, it is now possible to design such polymers for biomaterial applications.[2] At a nanoscale level, novel concepts such as self-assembly play a key role in developing performance protein polymers based on peptide molecular building blocks[3] (Figure 1). This research work illustrates a bread-board concept of the RSPP platform. These protein polymers, produced through molecular biological design using a bottom-up approach and fermentation, contain molecular peptide motifs and provide functional components that are assembled into protein-based structural/biomechanical scaffolds. The RSPPs permit the presence of regularly repeated natural sequence motifs that imply a propensity to adopt a regular structure and self-assembly. Here, we report and validate a novel, typical fermentation based cost-structure technology platform that exploits the natural structural scaffold derived from silk and elastin as a strong and unique base material.[4] In this study, we illustrate that this material, when periodically decorated with desired functional peptides at the genetic construct design level (for example, an antimicrobial or textile targeting or UV-protective agent), will introduce functional attributes in the designer protein polymer thereby opening new application opportunities for their use in biodefense, industrial biotechnology, and personal care, respectively.

Representative examples of natural, small peptide-based RSPP and their block copolymers (repeated amino acid sequences, using the one letter code, in parentheses) include elastin (GVGVP, VPGG, APGVGV), silk fibroin (GAGAGS), byssus (GPGGG), flagelliform silk (GPGGx), dragline silk (GPGQQ), GPGGY, GGYGPGS), collagen (GAPGAPGSQGAPGLQ, GAPGTPGPQGLPGSP), and keratin (AKLKLAEAKLELA). The relative environmental stability of these families of structural proteins, in combination with their biocompatibility, unique mechanical properties, and leverage for genetic control of sequence, provide the foundation on which one may exploit naturally derived RSPPs[5] for wide-ranging applications.[6] Natural protein polymers such as silk fibroins have been utilized to make high-performance fibers for a long time.[7] In combination with elastin, an ideal elastomer,[8] a synthetically designed RSPP[9] consisting of repeating motifs of these two proteins would reproduce defined properties of the natural counterparts along with properties found neither in the synthetic homoblock RSPP nor in the natural silk and elastin proteins (Figure 1).

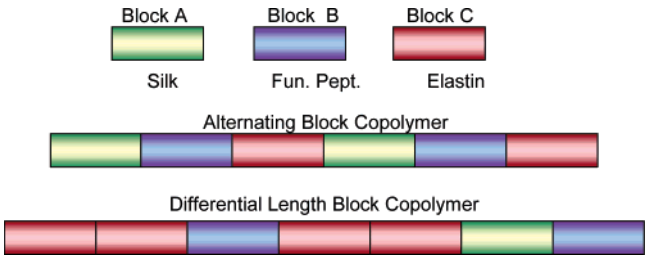

Figure 1. Designer RSPP materials: assembly line of designer protein-based performance materials with a bottom-up approach using natural repeat sequence motifs as building blocks, assembled in unique ways, to deliver specific benefits.

2. Experimental Procedures

2.1. Construction of Functional SELP47K. Silk-Elastin-Like Protein Polymer (SELP) consisting of four silk repeat peptides, seven elastin repeat peptides, and one lysine-modified elastin repeat peptide (SELP47K) is encoded by a 2652 base pair sequence present on a pUC-based plasmid under the control of a heat inducible lambda Pr promoter

* To whom correspondence should be addressed. E-mail: Manoj.Kumar@Danisco.com. Tel: 650 906-1184.

10.1021/bm060464a CCC: $33.50
Published on Web 08/19/2006

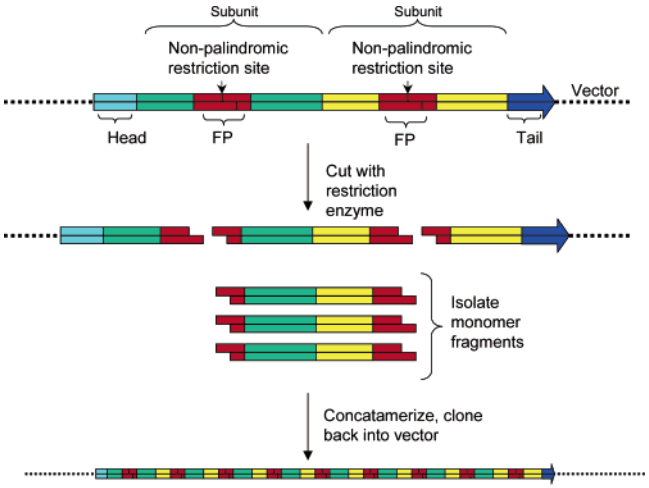

Figure 2. Illustration for the insertion of functional peptide sequences into SELP47K. FP-functional peptide.

and a selectable marker for kanamycin. A unique BamH1 restriction site was engineered into the 5′ "head" of the SELP47K coding sequence using Quick Change methodology. The generic method for inserting functional peptides into SELP47K is illustrated in Figure 2. A block monomer gene was synthesized incorporating peptide additions and unique nonpalindromic restriction enzyme sites. A subunit monomer was excised then reinserted into the vector backbone as concatamers followed by screening for polymers with the desired number of subunits.

2.2. Construction of AMP-SELP47K RSPP. Antimicrobial peptide MBI-28 WKLFKKIGIGAVLKVLTTGLPALKLTK (positively charged derivative of cecropin-bee melittin hybrid peptide) and cecropin A-melettin (CAM) hybrid KWKLFKKIGAVLKVL sequences were back translated into *Escherichia coli* DNA coding sequences using Vector NTI software. A hexamer tandem repeat was designed for each AMP, with individual AMPs being linked by glycine residue hexamers. 5′ and 3′ DNA sequences were added to the hexamers rendering the hexamer amenable to subcloning into the N-terminus of the SELP47K coding sequence with in-frame expression. Each AMP hexamer construct had a unique restriction enzyme cleavage site included within its sequence to facilitate screening and identification of correct constructs. AMP hexamer constructs were manufactured by Blue Heron Biotechnology (Bothell, WA) and provided in a pUC-based plasmid. Hexamer cassettes were subcloned into the SELP47K 3′ BamH1 site using T4 DNA ligase. Successful constructs were further verified for correctness using restriction enzyme/gel electrophoresis analysis, as well as DNA sequencing. Plasmids were used to transform *E. coli* MM294 using LB plates containing 50 ppm kanamycin, and single colonies were grown to produce frozen cryo vials, which were used as seed stocks for subsequent culturing and protein production.

The expression of AMP-SELP47K protein polymer was started with temperature induction by raising the fermentation temperature to 40 °C. Cell pastes were harvested by centrifuging the fermentation broth at the end of the fermentation. Both AMP-SELP47K fusion proteins were purified by homogenizing the cells using a French-Press. Homogenized cells were mixed with 0.5% polyethyleneimine (PEI) to flock out cell debris. The cell extract generated from centrifugation was mixed with ammonium sulfate (25% saturation) to precipitate AMP-SELP47K. Precipitated AMP-SELP47K fusion polymer was separated from the rest of the mother liquor and dissolved in MQ water. AMP-SELP47K was purified from its salt contents by dialysis and then lyophilized as a solid powder for storage.

2.3. Construction of Hexamer CBP-SELP47K and CBP-SELP47K (S2E1) RSPP. The cellulose binding peptide (CBP) sequence (TTHPQMLWQMST) was constructed in-house using PCR-driven phage display. The CBP peptide sequence was back translated into the *Escherichia coli* DNA coding sequence using Vector NTI software. A hexamer-tandem-repeat was designed using the CBP DNA sequence, with individual CBPs being linked by glycine residue quadtramers. Recombinant CBP-SELP47K plasmids were screened for the presence of the N-terminus hexamer CBP cassette using plasmid isolation and restriction enzyme analysis/gel electrophoresis. A plasmid was used to transform *E. coli* MM294 using LB plates containing 50 ppm kanamycin. Single colonies were picked and grown in 60 mL minimal medium with 2% glucose and 50 ppm kanamycin (500 mL fluted Erlenmeyer flasks, 30 °C, 250 rpm, 16 h). The cell culture was supplemented with glycerol (10% v/v), and 1.5 mL aliquots were placed in cryovials and stored at −80 °C.

Artificial gene synthesis was used to create a two-subunit version of the CBP-SELP47K-S2E1 in which each identical subunit contains a unique nonpalindromic restriction site. Specifically, all 13 SELP47K subunits contained one linear cotton-binding peptide incorporated between the C-terminal end of the silk region and the N-terminal end of the elastin region (region S2E1). Monomers were self-ligated using T4 DNA ligase. The original purified vector was added to the ligation mix with additional fresh ligase and incubated at 16 °C for an additional 24 h. The ligation mix was used to transform *E. coli* TOP10 cells. Resulting transformants were used to inoculate culture tubes containing 5 mL of Luria broth and an appropriate antibiotic. Tubes were incubated (16 h, 37 °C, 250 rpm). Plasmids were purified from the resulting cultures using a Plasmid Miniprep kit (Qiagen). Appropriate SELP47K-CBP conjugate gene constructs were subcloned into a vector containing the lambda Pr promoter and transformed into production host *E. coli* MM294. Fermentation and recovery of both CBP-SELP47Ks were carried out as described for AMP-RSPP.

2.4. P4-SELP47K RSPP Construction. Construction, analysis, and verification of the P4-SELP47K RSPP was similar to that of CBP-SELP47K-(S2E1). SELP constructs in which all polymer subunits contain two P4 (ALSYP) peptide sequences were made (Figure 2). Appropriate P4-SELP47K gene constructs were subcloned into a vector containing the lambda Pr promoter and transformed into production host *E. coli* MM294. Purified P4-SELP47K RSPP was made using the fermentation process described above and tested for UV protection efficacy studies.

2.5. Antimicrobial activity of AMP-RSPP. Antimicrobial activity of purified samples was assayed as follows: Samples of interest as well as AMP positive controls and a purified SELP47K negative control, were used. Positive controls were serially diluted 1:2 from 200 μg/mL to 1.56 μg/mL in Luria Broth (LB media) and consisted of cecropin A melittin (Sigma) and MBI-28 (synthesized in-house). *Escherichia coli* MG1655 and *Bacillus subtilis* 168 were used as Gram-negative and Gram-positive microbial targets. Five milliliter overnight cultures, grown from single colonies in LB, were diluted 1:250 in Terrific Broth (TB), and 100 μL aliquots were placed in duplicate in wells of sterile flat bottom 96-well microtiter plates. Uninoculated TB was also aliquoted as the control. Perimeter wells were not used but were instead filled with media so as to minimize "edge effects". An amount of 100 μL of the above dilutions of controls and samples was mixed with diluted bacterial aliquots, as well as with 100 μL of sterile TB as negative controls/blanks. Plates were incubated and humidified, at 37 °C, 250 rpm. The OD_{600} for each well was monitored hourly using a plate reader.

Purified CAM-SELP47K and MBI-SELP47K RSPP biomaterials were tested for their antimicrobial activity. Lyophilized material was dissolved in water at 1.25 mg/mL and used in a test tube based assay performed as follows: *Bacillus subtilis* 168 and *Escherichia coli* MG1655 were each grown from single colonies in 5 mL volumes of LB in test tubes, 37 °C, 250 rpm, 16 h. Cultures were diluted 1:500 in TB. Equal volumes of diluted culture and the purified AMP-SELP fusions described above were combined in sterile glass test tubes (1 mL total volume in 5 mL tubes), in duplicate, and incubated (37 °C, 250 rpm). Purified SELP47K was used as a negative control.

2.6. CBP-SELP47K RSPP Assay for Cellulose Binding Properties. All binding studies were carried using a European laundry detergent standardized protocol. Each experiment consisted of preparation of the cotton swatches and detergent, incubation of CBP-SELP47K with cotton

in European detergent, and determination of the amount of CBP-SELP47K bound to the cloth. A circular $^1/_4$ in. die punch was used to make cotton microswatches from EMPA 221 unsoiled cotton fabric (Testfabrics Inc.). Twenty-eight microswatches were washed for 15 min at 37 °C in 10 mL of filtered WFK-1 European laundry detergent (3.5 g/L, AATCC (American Association of Textile Chemists and Colorists) containing 15 grains per gallon (gpg) hardness (1.85 mM $CaCl_2$, 0.54 mM $MgCl_2$). The samples were washed using a DYNAL rotating mixer (40 rpm). The swatches were then rinsed in 3 gpg water hardness (0.37 mM $CaCl_2$, 0.108 mM $MgCl_2$) at 37 °C for 5 min (40 rpm) and then blotted dry on paper towels. Three concentrations of the RSPP proteins (CBP-SELP47K, 1.25, 0.84, 0.45, and 0 mg/mL; SELP47K, 1.35, 1.0, and 0.58 mg/mL) were made up in filtered WFK-1 European laundry detergent (3.5 g/L, 15 gpg hardness). A total of 900 μL of the diluted SELP proteins was then added to a 1.5 mL eppendorf tube containing 4 prewashed cotton microswatches. The tubes were mixed on a DYNAL rotary mixer (30 min, 40 °C, 400 rpm). The swatches were then rinsed 3 times in 1 mL of water containing 3 gpg hardness (5 min, room temperature, shaking). The swatches, supernatant, and rinses were all analyzed for the presence of SELP47K using the BCA protein assay (Pierce). The BCA assay was modified appropriately to analyze the solid cotton swatches. For testing the cotton-binding properties of hexamer CBP-SELP47K and CBP-SELP47K-S2E1, swatches were prepared in the same manner as that described in the previous experiment. Forty washed swatches were placed in a 48-well microtiter plate such that each variable (CBP-, S2E1, and 47K control) was exposed to 0, 1, 2, 3, 4, and 5 swatches each. SELP47K stock solutions (SELP47K, 1 mg/mL; CBP-SELP47K, 0.75 mg/mL) were prepared in filtered WFK-1 European laundry detergent (3.5 g/L, 15 gpg hardness). An amount of 200 μL of the SELP stock solutions was added to the wells of the microtiter plate, which contained the washed swatches. The SELP proteins were incubated with the swatches (40 °C, 30 min, 240 rpm). The supernatant was then removed from the wells, and the swatches rinsed 3 times in 3 gpg water (600 μL, 5 min shaking). The swatches were analyzed in the manner described in the previous binding experiment.

2.7. Assay for Protection against UVB Exposure. Two duplicate sets of cultured human fibroblasts were exposed to six concentrations of the P4-SELP47K. The first set of cells was exposed to approximately 50 mJ/cm^2 of UVB, followed immediately by the application of either the test material, 20 μM Trolox (an antioxidant, used as a positive control), or left untreated (untreated controls). The second set of cells did not receive a dose of UVB and was only exposed to either the P4-SELP47K, Trolox, or left untreated. Changes in cell viability were then determined 48 h post material application via an MTT assay. Human dermal fibroblasts when exposed to a dose of UVB light (approximately 50 mJ/cm^2) typically show a reduction in the number of viable cells by 50% at 48 h post UV exposure. The mean MTT absorbance value for the negative control cells was calculated and used to represent the 100% value for cell number. The individual MTT values from cells undergoing various treatments was then divided by the mean value for the negative control cells and expressed as a percent to determine the change in cell number caused by each treatment.

2.8. MatTek Full Thickness Tissue Skin Model Study. Three tissues were allowed to incubate for 24 h at 37 ± 2 °C and 5 ± 1% CO_2. Following incubation, the assay medium was replaced with 5 mL of fresh medium (37 ± 2 °C) prior to application of samples. After incubation with the samples, three tissues were transferred to a 24-well plate containing 300 mL of PBS per well. An amount of 50 μL of test material (0.14% P4-SELP47K in PBS) was applied to one tissue, while the remaining two tissues were treated with 50 μL of PBS + BSA (0.14% final BSA concentration). One of the BSA treated tissues was set aside and used as a non-UVB exposed control while the remaining tissue treated with BSA and the P4-SELP47K treated tissue were irradiated with an approximate dose of 300 mJ/cm2 UVB. Immediately after UVB irradiation, the tissues were rinsed with PBS and 50 μL of fresh material was applied to the tissues and the tissues were transferred to a 6-well plate containing 5 mL of fresh medium per well. The tissues were then incubated at 37 ± 2 °C and 5 ± 1% CO_2 for 24 h. After incubation, the cell culture medium was collected and stored at −75 °C until analyzed. The tissues were rinsed with phosphate buffered saline to remove any residual test material and then cut into thirds. One-third of the tissue was used for an MTT assay to determine changes in tissue viability, another third was used to assay for changes in fibulin-5, MMP1, PGE_2, and p53 via western analysis, and the remaining third was used to assay for the presence of DNA ladders.

For the MTT assay, the tissue was weighed and then transferred to a 24-well plate containing 300 mL of assay medium supplemented with MTT (1 mg/mL) and allowed to incubate for 3 ± 0.25 h at 37 ± 2 °C and 5 ± 1% CO_2. After the incubation, the tissues were rinsed then placed into 2 mL of 2-propanol to extract the reduced MTT from the tissues, following which, absorbance of the sample was read at 540 nm. Individual absorbance values were normalized to the weight of the tissue. Tissues were prepared for western blot analysis as follows. The tissue portion was placed into 1.5 mL centrifuge tubes containing 0.3 mL of RIPA buffer (50 mM TRIS, pH 7.4, 150 mM NaCl, 1 mM PMSF, 1 mM EDTA, 5 μg/mL aprotinin, 5 μg/mL leupeptin, 1% Triton X-100, 1% sodium deoxycholate, 0.1% SDS) and homogenized. After centrifuging the homogenates at 14 000 × g for 5 min, the supernatant was transferred to a new tube while the pellet containing insoluble debris was discarded. The protein concentration of the homogenate was determined using a BCA protein assay. Western blot work was done using standard protocols and using commercially available anti-fibulin-5 and anti-p53 antibodies. The secondary antibody (conjugated with an alkaline phosphatase enzyme) was then incubated with the membrane in 10 mL of TBST with 0.5% nonfat powdered milk. The membrane was incubated for 1 h at room temperature, washed 3 times with TBS (1 × 15 min, 2 × 5 min) and exposed to film. The films were then subjected to densitometric analysis to quantify changes in the markers of interest. Densitometric measurements are expressed in arbitrary optical density units (OD). Mean OD values for each treatment were then calculated, and treatments were compared using a one-way ANOVA.

A series of PGE_2 standards were prepared ranging from 7.8 to 250 pg/mL. An ELISA plate was prepared by designating two wells each for the following: total activity (TA) wells, nonspecific binding (NSB) wells, maximum-binding (MB) wells, and substrate blank wells (B_0). An amount of 150 μL of tissue culture medium was added to the NSB wells while 100 μL of medium was added to the B_0 wells. A total of 100 μL of standard or sample was then added to the respective wells followed by the addition of 50 μL of the PGE_2 alkaline phosphatase conjugate (except the TA and B_0). Next, 50 μL of PGE_2 alkaline phosphatase antibody solution was added to each well (except the TA, NSB, and SD wells). The plate was then covered and incubated at 2−8 °C for 24 h. After the incubation, each well was washed three times with 400 μL of wash buffer. An amount of 5 μL of PGE_2 alkaline phosphatase conjugate was added to the TA wells, and then 200 μL of pNPP substrate was added to all wells. The plate was then covered and incubated at 37 ± 2 °C for 1 h. At the end of the incubation period, 50 μL of stop solution was added to each well and the plate was read at 405 nm using a wavelength correction at 540 nm. For this ELISA-based assay, the absorbance values for the known standards were used to generate a standard curve. The values for the unknown samples were then determined from this standard curve, and the means for each treatment will then be compared using a one way ANOVA.

The remaining tissue portions were placed into 1.5 mL centrifuge tubes containing 180 μL of Lysis Buffer and the protocol for DNA laddering was followed as detailed in the Qiagen kit (Qiagen, DNEasy Kit). Extracted DNA was quantified via a fluorometric assay using Hoechst 33258 dye (0.006 mg/mL in assay buffer), and the fluorescence intensity of each well was determined using an excitation wavelength of 355 nm and an emission wavelength of 485 nm. Aliquots of equal amounts of DNA from each tissue were resolved on a 2% agarose gel

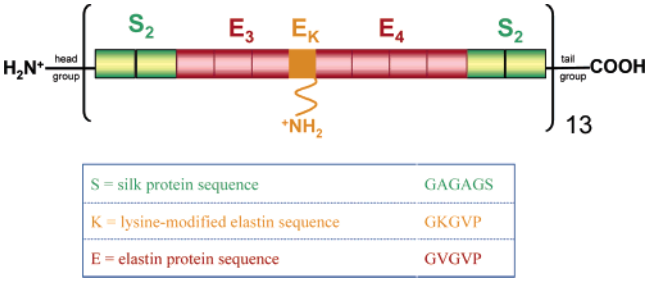

Figure 3. Designer RSPP materials: unit block structure of Silk-Elastin-Like Protein polymer (SELP47K).

containing 0.5 μg/mL ethidium bromide. The DNA was visualized using a UV transilluminator and photographed.

3. Results

3.1. RSPP Design and Properties. In this study, we used designer blocks of silk fibroin (S = GAGAGS) and elastin (E = GVGVP) with a unique amino acid sequence to create a specific RSPP named SELP47K (unit block structure, Figure 3), which can provide novel chemical, biological, and functional attributes, while maintaining the physical properties of the structural blocks.

By exploiting the degeneracy of the genetic code such that nonidentical DNA encodes adjacent, identical oligopeptide block sequences, we have specifically designed these genes to avoid recombinatorial deletion and have been able to produce and stably maintain repetitive genes and gene products in microorganisms.[10,11] Using precise sequence design and gene construction, we have been able to maintain recombinant genes of over 5000 base pairs in *E. coli* using a strain deficient in the deletion mechanism of homologous recombination, particularly DNA-modifying functions.[12] The design principles have also included low-energy barrier energetics, high reaction-, regio- and stereospecificity and local control of the dielectric environment.

SELP47K consists of four silk repeat peptides, seven elastin repeat peptides, and one lysine-modified elastin repeat peptide. Substitution of one valine, by a lysine, in one individual unit of elastin imparts cross-linking functionality and also increases the polymer's water solubility.

SELP47K was chosen as the protein polymer block unit for its appropriate water solubility. The use of higher units of silk repeat peptides resulted in a water insoluble polymer, whereas higher elastin repeat peptide units led to a polymer with weaker mechanical properties. Thirteen repeats of SELP47K resulted in a polymer with the highest fermentation yield. Attempts to make a polymer of greater than 100 kD molecular weight were less successful. Protein polymers of sizes between 60 and 80 K were found to be best both in terms of genetically engineering the DNA multimer as well as producing the polymer in good yield (>1 g/L) by fermentation.

SELP47K offers unique properties such as self-assembling nanofilamentous structures (Figure 4) in film, fiber, or in a hydrogel form, has mechanical strength, and other unique physical properties[10] creating a versatile structural scaffold.

The following three examples represent ordered block-based incorporation of both multifunctional biomolecular peptides and naturally occurring structural biomechanical peptides into the self-assembling SELP47K RSPP scaffold. The designer protein polymers thus created have resulted in the development of a versatile functional RSPP platform technology with numerous possible applications.

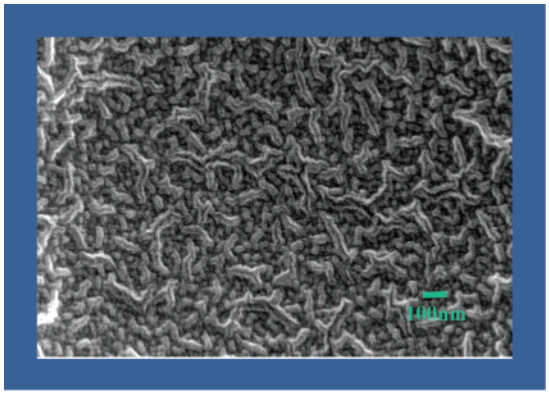

Figure 4. Designer RSPP materials: self-assembling nanofilamentous structure of SELP47K in a casted film as observed by SEM (60 000× magnification). Average diameter of rod shape nanofilaments is between 20 and 30 nm.

3.2. RSPP Applications in Biodefense. The first example illustrates the conjugation of antimicrobial peptides (AMPs) with the RSPP.[13] AMPs serve as a nonspecific defense system complementing the highly specific cell-mediated immune response. These peptides, present on epithelial surfaces and on phagocytic cells, are mobilized shortly after microbial infection. They act rapidly to neutralize a broad range of microbes.[13] In recent years, hundreds of antimicrobial peptides have been isolated, designed de novo, and synthesized (http://www.bbcm.univ.trieste.it/~tossi/pag1.htm). Although more than one mechanism of action has been proposed in the literature for them, the carpet mechanism model, which involves nonspecific membrane permeabilization by AMPs, is relevant for this work.[14] There are examples in the literature that support the concept that immobilized AMPs function biologically in a manner that is consistent with the free peptides as the biocidal moiety providing the basis for creating natural AMPs conjugated to RSPPs using the SELP47K structural scaffold[15,16] (Figure 5a).

Purified AMP-SELP47K was analyzed using SDS gel electrophoresis and mass spectrometry (Figure 5b). An antimicrobial activity assay (Figure 5c), using both *E. coli* and *Bacillus subtilis* cultures, showed that after 4 h of incubation, tubes containing AMP-SELP47K RSPP had significantly less growth compared to those containing control SELP47K confirming the growth inhibitory and antimicrobial properties of the AMP-RSPP (parts d and e of Figure 5). Preliminary work to compare the efficacy of AMPs in protein polymer vs free peptide showed that the free peptide was 100-fold more efficacious in its inhibition of bacterial growth than the equivalent AMP present in the polymer (data not shown). Figure 5c suggests that CAM was as effective as MBI in inhibiting the growth of both Gram-positive and Gram-negative bacteria.

3.3. RSPP Applications in Industrial Biotechnology. The second example illustrates creating functional RSPPs with a cotton-binding peptide (CBP). The CBPs were derived from screening a library of peptides under typical laundry wash conditions (data not shown). SELP47K and six repeats of the CBP (TTHPQMLWQMST), hereafter referred to as hexamer CBP-SELP47K, were conjugated and designed to bind to cotton using European detergent standards. Therefore, it can be used to attach a wider variety and greater amounts of agents to cotton materials as they are sustained through a wash cycle. Construction, analysis, and verification of the hexameric repeating CBP at the N-terminus of SELP47K were performed as described for AMP-RSPP. CBP-SELP47K-S2E1, in which each protein polymer scaffold subunit contained one cotton-binding peptide

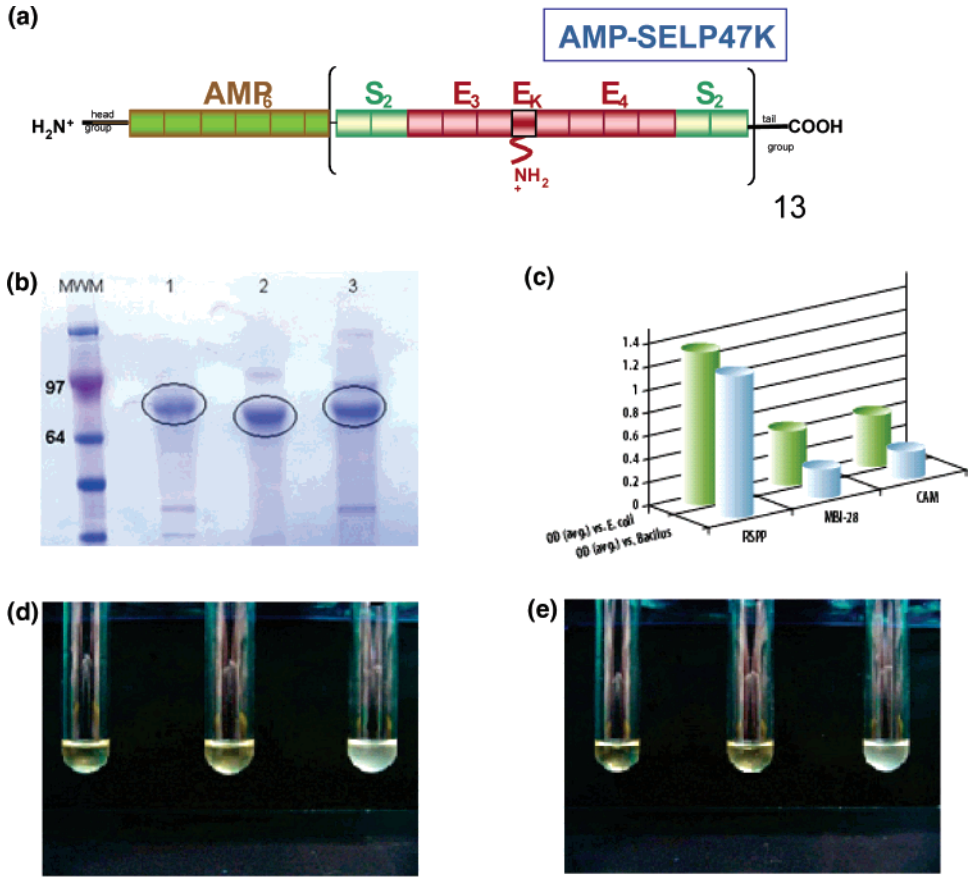

Figure 5. AMP-SELP47K RSPP study: (a) Unit block structure of AMP-SELP47K RSPP. (b) 1-D gel of purified RSPP and antimicrobial RSPP fusion proteins. Lane 1: CAM hex. at the N-term of SELP47K. Lane 2: SELP47K. Lane 3: MBI-28 hex. at the N-term of SELP47K. (c) Antimicrobial activity of AMP-SELP47K compared to SELP47K. (d) Growth inhibition in tubes: *E. coli* (left to right, CAM-SELP47K, MBI-SELP47K, SELP47K control). (e) Growth inhibition in tubes: *B. subtilis* (left to right, CAM-SELP47K, MBI-SELP47K, SELP47K control).

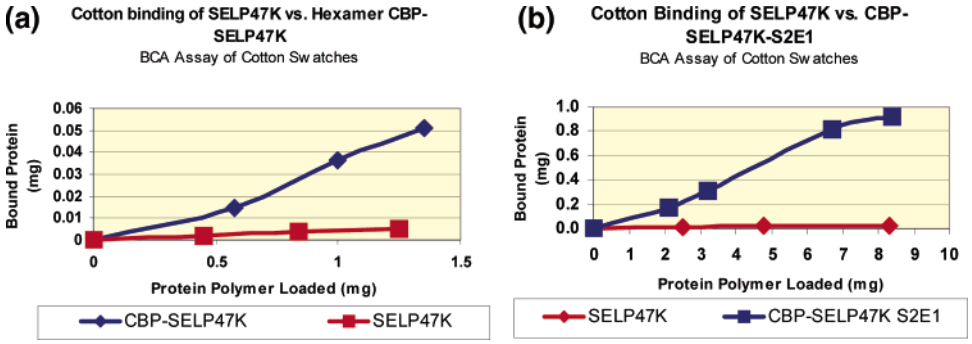

Figure 6. CBP-SELP47K and CBP-SELP47K-(S2E1) RSPP binding to cotton swatches under European detergent washing conditions. (a) The cotton-binding activity of hexamer CBP-SELP47K is compared to that of native SELP47K. The concentration of protein bound to the swatch is determined based on the BCA protein assay. (b) The cotton-binding activity of CBP-SELP47K-S2E1 is compared to that of native SELP47K. This assay is a dose response assay in which the cotton (substrate) concentration is held constant and the protein polymers concentration is varied.

sequence, was also generated. Both purified CBP-SELP47K RSPPs variants were analyzed using SDS gel electrophoresis and mass spectrometry (data not shown).

The cotton-binding properties of CBP-SELP47K were compared to SELP47K in two different assays. One assay was a dose response assay in which the cotton (substrate) concentration was held constant and the protein polymer concentration was varied. The second experiment was one in which the cotton concentration varied and the SELP47K concentration was held constant. All binding studies were carried out in European laundry detergent. Both CBP-SELP47K RSPPs were assayed for cellulose/cotton (substrate) binding properties, in two different assays, using SELP47K RSPP as the control. In the assay in which the cotton concentration was held constant and the hexamer CBP-SELP47K concentration varied, the cotton-binding activity of hexamer CBP-SELP47K, when compared to that of native SELP47K, was significantly greater (Figure 6a). The bound protein was eluted from the cotton and run on a SDS gel to confirm that the eluted protein was indeed hexamer CBP-SELP47K (data not shown). The CBP-SELP47K-S2E1 conjugate showed improved cotton binding compared to the hexamer CBP-SELP47K because of the likely reason that both the total number of cotton-binding peptides doubled within the polymer and the cotton-binding peptide appeared periodically throughout this conjugate (Figure 6b). More than 10% of CBP-SELP47K-S2E1 bound to the cotton in this assay.

(a)

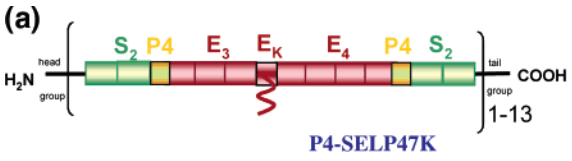

(b)

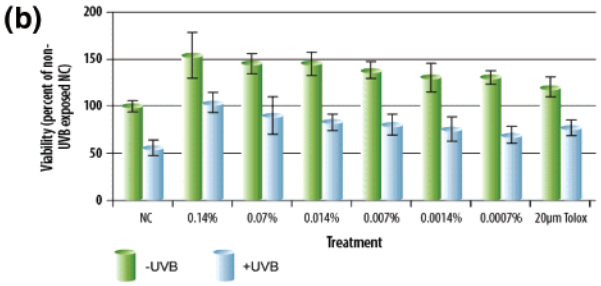

(c)

Treatment	24 hour pretreatment with P4-SELP47K	P4-SELP47K present during UVB exposure	P4-SELP47K Present for 48 hours after UVB exposure
T1	+	-	+
T2	+	+	+
T3	-	-	+
T4	-	+	+

(d)

Treatment	Percent Viability
No UVB	100 +/- 27
UVB	79 +/- 9
T1+ 0.14% P4-SELP47K	122 +/- 20
T1+ 0.014% P4-SELP47K	85 +/- 7
T2 + 0.14% P4-SELP47K	126 +/- 25
T2 + 0.014% P4-SELP47K	78 +/- 4
T3 + 0.14% P4-SELP47K	97 +/- 14
T3 + 0.014% P4-SELP47K	88 +/- 17
T4 + 0.14% P4-SELP47K	121 +/- 19
T4 + 0.014% P4-SELP47K	86 +/- 6

(e)

Treatment	RFU/Viability
No UVB	0.031
UVB	0.057
T1+ 0.14% P4-SELP47K	0.038
T1+ 0.014% P4-SELP47K	0.038
T2 + 0.14% P4-SELP47K	0.032
T2 + 0.014% P4-SELP47K	0.035
T3 + 0.14% P4-SELP47K	0.039
T3 + 0.014% P4-SELP47K	0.053
T4 + 0.14% P4-SELP47K	0.026
T4 + 0.014% P4-SELP47K	0.052

Figure 7. Photoprotective RSPP study: (a) Unit block structure of P4-SELP47K RSPP. (b) UVB protective effect of P4−SELP47K RSPP. (c) Experimental setup to confirm UVB protective effect of P4-SELP47K with its presence in pre- and post-UVB dosage (+ indicates that the material was present, − indicates that the material was absent). (d) In vitro study using MTT assay to monitor the effect of P4-SELP47K on cell viability in pre- and post-UVB insult using human skin fibroblast cells. (e) In vitro study using DCF assay to monitor the effect of P4-SELP47K on cell viability in pre- and post-UVB insult using human skin fibroblast cells.

The cotton-binding ability of the two CBP-SELP47K RSPPs was also assayed at different cotton concentrations. The amount of CBP-SELP47K that bound to cotton increased with increasing cotton concentration. Equal amounts of hexamer CBP-SELP47K bound to each swatch regardless of the number of swatches present in the reaction, indicating that hexamer CBP-SELP47K had saturated all the binding sites available on the cotton swatches (data not shown).

3.4. RSPP Applications in Personal and Health Care. The third example illustrates potential applications in personal and health care areas. A radio protective functional RSPP with peptide P4 (ALSYP; a naturally derived peptide-based UV-protective agent, from Bowman Birk Inhibitor, BBI) was designed to generate P4-SELP47K[17] (Figure 7a). Construction, analysis, and verification of P4-SELP47K, where two P4 peptide motifs were incorporated in each SELP47K unit, were done as described for the CBP-SELP47K-S2E1. First, a human skin fibroblast cell culture model was used to assess the UV-protective properties of P4-SELP47K, by measuring cell survival after UVB exposure using a MTT assay. Increasing concentrations of P4-SELP47K inhibited the decrease in the number of viable cells induced by UVB exposure (Figure 7b). This effect was most prominent at the highest concentration of P4-SELP47K RSPP used (0.14%), where the level of cell viability is nearly identical to the untreated −UVB exposed cells and almost twice the level of the untreated +UVB exposed cells. As the concentration of P4-SELP47K decreased, so did the apparent protective effect although even at the lowest level of the material, 0.0007%, the number of viable cells was still slightly greater than the +UVB untreated controls (69% vs 55%, respectively). In the absence of UVB light, P4-SELP47K was found to stimulate cell proliferation in a dose-dependent manner. At the highest concentration tested (0.14%), the number of viable cells in the −UVB condition was 54% greater than the −UVB untreated cells. This stimulation effect was apparent over the entire range of P4-SELP47K concentrations tested and suggests two possibilities for the mechanism by which P4-SELP47K may exert its UV-protective effect. P4-SELP47K could protect the cells by limiting the amount of damage or facilitating the repair after UVB-induced damage, thus allowing the population of viable cells to be better maintained than in the untreated condition. On the other hand, P4-SELP47K may provide little or no protection against the UVB-induced damage but rather function to stimulate the surviving cells to proliferate at a faster rate than the untreated cells. While either explanation could be argued, the increase in the number of viable cells was greater between the +UVB untreated and the +UVB with 0.14% P4-SELP47K RSPP conditions (50% viability vs 100% viability, respectively, double the number of viable cells) than in the −UVB untreated and the −UVB test material conditions (100% viability vs 150% viability, respectively, only a 50% increase), suggesting that, in the presence of P4-SELP47K, with UVB insult, there is a greater increase in the number of viable cells than can be accounted for solely by the cell proliferation stimulating action of P4-SELP47K. This observation strengthens the first explanation that P4-SELP47K RSPP does indeed provide protection against UVB-induced damage.

Since these results suggested that the P4-SELP47K RSPP is capable of improving cell survival when applied after UVB exposure, we tested whether treatment with P4-SELP47K before or during UVB exposure would provide any additional survival benefit by measuring cell survival 48 h after UVB insult. Four different treatment regimens (Figure 7c) were employed using different combinations of pretreatment prior to or during UVB exposure. We also incorporated the use of 2′,7′-dichlorodihydrofluorescein diacetate (DCF), which when loaded into cells becomes fluorescent upon exposure to the reactive oxygen species (ROS) generated during UVB exposure.[18,19] As seen in

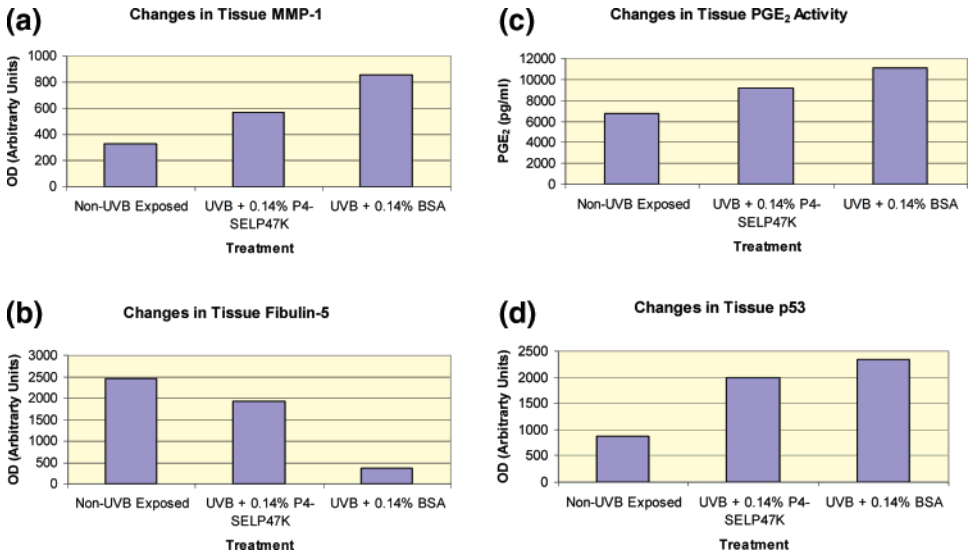

Figure 8. Photoprotective RSPP follow-up study: (a) Changes in skin tissue MMP-1 levels upon UVB exposure in the presence and absence of P4-SELP47K. (b) Changes in skin tissue fibulin-5 levels upon UVB exposure in the presence and absence of P4-SELP47K. (c) Changes in skin tissue PGE2 levels upon UVB exposure in the presence and absence of P4-SELP47K. (d) Changes in skin tissue p53 levels upon UVB exposure in the presence and absence of P4-SELP47K.

Figure 7c, the UVB protective effect of P4-SELP47K was improved when the material was present both before and/or during UVB exposure. Treatment 3, which is identical to the treatment regimen used in the previous study, shows similar results with respect to the MTT assay (Figure 7d). At the 0.14% concentration, cell viability after UVB exposure is again close to 100% after the UVB (vs 104% in Figure 7b), and at the 0.014% concentration, it is 88% (vs 83% in Figure 7b). At both concentrations, the extent of cell survival is greater than the extent of cell survival in the untreated cells exposed to UVB. In the DCF assay, which estimates the amount of oxidative damage occurring within the cell as a result of the UVB exposure, a higher ratio indicates a greater extent of ROS formation within the cell (Figure 7e). Again, with respect to treatment 3, both concentrations of the P4-SELP47K RSPP reduced the amount of ROS formed when compared to the ROS formation in untreated cells exposed to UVB. These results confirm observations from the first study and further support that P4-SELP47K can provide UVB protection. For treatments 1, 2, and 4, it appeared that P4-SELP47K at the 0.14% concentration either for 24 h before exposure or just during UVB exposure provides a similar level of protection.

To further explore the mechanism of P4-SELP47K UVB protective abilities, we used the MetTak human skin full-thickness tissue model (EFT 200) and tested changes in tissue viability,[20,21] MMP1,[22−24] fibulin-5,[25,26] PGE_2,[27,28] DNA laddering,[29,30] and up-regulation of p53[31,32] in response to UVB irradiation in the presence and absence of 0.14% solution of P4-SELP47K in PBS applied topically. For positive control, a 0.14% BSA solution was topically applied to the tissue prior to UVB exposure.

UVB exposure was observed to reduce tissue viability by 31% in the tissue treated topically with BSA. However, the tissue treated with P4-SELP47K had only a 20% reduction in viability supporting the previous results of skin fibroblast studies (data not shown). P4-SELP47K was also able to reduce the level of induction of MMP1 by 33% upon UVB exposure (Figure 8a). In tissues treated with BSA prior to UVB exposure, the amount of fibulin-5 decreased by 85%. However, this decrease was significantly attenuated (22.5%) in tissues treated with P4-SELP47K (Figure 8b).

PGE2 release in the P4-SELP47K treated tissue was only 1.36 times that of UVB untreated tissue compared to a 1.65-fold increase in the BSA treated tissue (Figure 8c). UVB treatment was observed to induce the expression of p53 (2.7-fold) and the formation of DNA ladders in the BSA treated tissue. In contrast, UVB induced expression of p53 was reduced to 2.3-fold in tissue treated with P4-SELP47K (Figure 8d), while the formation of DNA ladders was almost completely blocked (data not shown).

4. Discussion

Over the years, block copolymers have attracted a great deal of interest because they offer a unique platform for the development of materials in diverse applications. RSPPs described in this paper are the result of knowledge-based polymer design, relying on the fact that repeated sequences adopt specific structural motifs that provide the basis for polymer formation. RSPPs are similar to a chemically polymerized block of copolymers but do not have any heterogeneity. They are unique, defined, monodispersed, and have molecular weights generally between 30 and 250 kD. Using RSPP platform technology, we have described creating designer functional protein polymers using functional peptides and embedding them into biomechanical natural protein-based scaffolds to create opportunities for the development of protein-based materials for multiple applications.

Placement of functional peptides in the SELP47K protein polymer scaffold was based upon the specific function and properties of the peptides. Antimicrobial peptides were positioned as multimers in front at the N-terminus, whereas the UV-protective functional peptide P4 was positioned internally between the silk and elastin units. Attempts to place functional peptides at the C-terminus were not successful. AMPs were specifically designed as hexamers at the N-terminus of the protein polymer to allow some degree of freedom for their action. Hexameric AMP constructs were used to deliver an improved antimicrobial peptide concentration per polymer molecule. On the other hand, the P4 peptide, which is known for its UV-protective efficacy from within its parent molecule, BBI was thus incorporated internally within the protein polymer.

Furthermore, two P4 peptides per SELP47K monomer provided a total of 26 peptides dispersed periodically throughout the polymer. It was anticipated that this should result in a highly efficacious UV-protective polymer and was supported by the results obtained in the UV-protective study. A cotton-binding peptide was incorporated both at the N-terminus and internally throughout the polymer to find the effect and efficacy of both, the number of peptide units in the polymer and their position in the polymer. CBP placed as a hexameric multimer (6 CBP units) at the N-terminus showed about 20× lower binding capacity to cotton than to 13 CBP units placed periodically inside the polymer. These studies indicate that placement of certain functional peptides periodically throughout the polymer is more desirable for certain activities, such as binding and targeting.

We have shown that functional protein polymer technology offers making biobased performance materials at a fermentative protein production cost structure. For example, our technology offers the means to make peptides at a cost structure that is about 10 000 times less expensive than peptides made today using synthetic methods. A typical cost of 1 g of synthetic pentapeptide is about $15 000, whereas it is feasible to make the same amount of peptide and protein content at $1.50 using the RSPP technology.

The antimicrobial properties of CAM-SELP47K and MBI-28-SELP47K were verified using both *E. coli* and *B. subtilis* cultures (Figure 5). CAM and MBI-28 are both cecropin-derived antimicrobial peptides except that MBI-28 is a much longer peptide with higher effective positive charge. CAM and MBI-28 were selected for their known broad efficacy against both Gram-positive and Gram-negative bacteria. Both antimicrobial peptides were further selected on the basis of having no cysteines as attempts to make protein polymers with cysteines were less successful. Figure 5e suggests that CAM was equally effective as MBI for both Gram-positive and Gram-negative bacteria. Comparison of free peptide vs peptide in the polymer showed that free peptide was 100-fold more efficacious in its inhibition of bacterial growth than an equivalent antimicrobial peptide present in the polymer. This result was not unexpected as antimicrobial peptides when constrained as a part of protein polymers have a reduced degree of freedom toward the bacterial cell. However, use of free antimicrobial peptides for developing antimicrobial materials is not viable due to its cost of synthesis and difficulty of immobilization onto a material. Protein polymers containing antimicrobial peptides offer the possibility of producing the peptides by fermentation at a desired cost structure as discussed above and appropriately assimilating them into a composite material that is capable of showing excellent antimicrobial efficacy. The most remarkable property of AMPs is that development of microbial resistance against them is uncommon.[33] For this reason, using AMPs in creating antimicrobial RSPP-based materials offers long-term efficacy and stability against microbial infection. It is thus conceivable that AMP-RSPPs may be successfully incorporated into textiles, filters, surgical masks and gowns, protective garments, garments designed for biological warfare defense, wound dressings, skin cream, and coatings to provide a hygienic surface to protect against microorganisms.

The cotton-binding activity of hexamer CBP-SELP47K was shown to be significantly greater than that of native SELP47K. CBPs, unlike cellulose binding modules (CBMs), can be made application specific and can be tailored to meet requirements for pH, conductivity, presence of detergent, solvents, and so forth, thus making the use of CBP-RSPP advantageous over the use of CBMs for targeting molecules to cotton substrates.[34] Applications toward targeting efficacy using peptides as evident in this example using CBP are dependent on both the number of peptides present in the polymer as well as their placement in the polymer architecture. We find that the cotton-binding affinity of CBP-SELP47K-S2E1 is about 20× more than that of hexamer CBP-SELP47K. It is thus anticipated that incorporation of CBP-RSPP into, for example, fabrics and textiles or cotton gauge dressing would render these materials more amenable to specific targeting and work as delivery agents to access a desirable target site. Other applications may include fabric care and development of detergent formulations suitable for improved cleaning of cotton-based clothing. The results with CBP-RSPP further confirm the utility of designer protein-based materials for possible targeting applications exemplifying potential uses in white (industrial) biotechnology.

Data from Figures 7 and 8 demonstrate the effectiveness of P4-SELP47K as a UV-protective agent and its possible use in reduction and prevention of photoaging of human skin. The P4 peptide, which is part of the chymotrypsin loop of BBI, was found to be a functional and effective UV-protective agent when placed in a periodic fashion in the SELP47K structural scaffold because SELP47K provided a constrained structure (as a result of β-sheet formation) as by the chymotrypsin loop of BBI. The P4 functional RSPP is designed with the idea that it may be used in applications such as incorporation into textiles, wound dressings, and skin creams to protect human skin from UV radiation and chronological photoaging. Such engineered biopolymers would closely simulate natural polymers but would also be capable of protecting human/animal skin from exposure to UV radiation. This example provides credence to the RSPP technology for making designer protein-based materials in human care applications.[35]

This study further suggests that the SELP47K scaffold is a versatile and mechanically robust structural protein polymer platform where functional peptides can be placed based upon their functionality considerations to make performance materials.

Materials made of naturally occurring peptide building blocks are being studied for applications such as direct tissue replacement and engineering.[36] Genetically engineered elastin-like homoblock polypeptides are being made for applications in cartilage tissue repair and targeted drug delivery.[37] Furthermore, advances in this field include both control of assembly and function using homodiblock copolypeptides.[38] Amphiphilic molecules that have repeating peptide motifs and hydrocarbon chains have been designed to form hydrogels having cylindrical nanofibers.[39] Synthesis and self-assembly of hybrid triblock copolymers, combining both π-conjugated man-made polymers and polypeptide blocks have been shown to exhibit both photoactivity and electroactivity.[40] In addition, hybrid block copolymers containing pegylated peptides that respond to specific cellular signals such as adhesion and migration of endothelial cells have been developed.[41] The RSPP platform technology described in this paper presents a new way to design, develop, and produce new protein-based performance materials as compared to hybrid peptide−synthetic organic materials currently being researched for biomaterials and other relevant market opportunities.[42]

Acknowledgment. We thank Dr. Roopa Ghirnikar for her editorial help.

References and Notes

(1) Langer, R.; Tirell, D. A. *Nature* **2004**, *428*, 487−492.
(2) Ratner, B. D.; Bryant, S. J. *Annu. Rev. Biomed. Eng.* **2004**, *6*, 41−75.
(3) Zhang, S. *Nat. Biotechnol.* **2003**, *21*, 1171−8.

(4) Collier, C. D.; Cuevas, W. A.; Kumar, M. U.S. Patent Application Publication No. US 0234609A1, 2004.
(5) Tirrell, D. A. *Nature* **1997**, *336*−*337*, 339 and refereneces therein.
(6) Wright, E. R.; Conticello, V. P. *Adv. Drug Delivery Rev.* **2002**, *54*, 1057−73.
(7) Horan, R. L.; Antle, K.; Collette, A. L.; Wang, Y.; Huang, J.; et al. *Biomaterials* **2005**, *26*, 3385−3393.
(8) Urry, D. W.; Hugel, T.; Seitz, M.; Gaub, H. E.; Shieba, L.; et al. *Philos. Trans. R. Soc. London, Ser. B* **2002**, *28*, 357 (1418), 169−84.
(9) Cappello, J. *Trends Biotechnol.* **1990**, *8*, 309−311
(10) Ferrari, F.; Cappello, J. in *Protein-Based Materials*; Birkhauser: Boston, MA, 1997; Chapter 2.
(11) Kumar, M.; Cuevas, W. A. U.S. Patent Application Publication No. US 2004/0180027A1, 2004.
(12) Kumar, M.; Mazeaud, I.; Christiano, S. P. U.S. Patent Application Publication No. US 2004/0228913A1, 2004.
(13) Hancock, R. E. W. *Lancet Infect. Dis.* **2001**, *1*, 156−164.
(14) Shai, Y. *Biopolymers* **2002**, *66*, 236−248.
(15) Haynie, S. L.; Crum, G. A.; Doele, B. A. *Antimicrob. Agents Chemother.* **1995**, *39*, 301−307.
(16) Sal-Man, N.; Oren, Z.; Shai, Y. *Biochemistry* **2002**, *41*, 11921−11930.
(17) Dittmann, K. H.; Gueven, N.; Mayer, C.; Rodemann, H. P. *Protein Eng.* **2001**, *14*, 157−160.
(18) Carini, M.; Aldini, G.; Piccone, M.; Facino, R. M. *Farmaco* **2000**, *55*, 526−34.
(19) Chan, W.; Wu, C. C.; Yu, J. S. *J. Cell. Biochem.* **2003**, *90*, 327−338.
(20) Rijnkels, J. M.; Whiteley, L. O.; Beijersbergen van Henegouwen, G. M. *Photochem. Photobiol.* **2001**, *73*, 499−504.
(21) Ma, W.; Wlaschek, M.; Tantcheva-Poór, I.; Schneider, L. A.; Naderi, L.; et al. *Clin. Exp. Dermatol.* **2001**, *26*, 592−599.
(22) Brenneisen, P.; Oh, J.; Wlaschek, M.; Wenk, J.; Briviba, K.; et al. *Photochem. Photobiol.* **1996**, *64*, 877−885.
(23) Brenneisen, P.; Wlaschek, M.; Schwamborn, E.; Schneider, L. A.; Ma, W.; et al. *Biochem. J.* **2002**, *365*, 31−40.
(24) Petersen, M. J.; Hansen, C.; Craig, S. *J. Invest. Dermatol.* **1992**, *99*, 440−444.
(25) Nakamura, T.; Lozano, P. R.; Ikeda, Y.; Iwanaga, Y.; Hinek, A.; et al. *Nature* **2002**, *415*, 171−175.
(26) Kadoya, K.; Sasaki, T.; Kostka, G.; Timpl, R.; Matsuzaki, K.; et al. *Br. J. Dermatol.* **2005**, *153*, 607−612.
(27) Podda, M.; Traber, M. G.; Weber, C.; Yan, L. J.; Packer, L. *Free Radical Biol. Med.* **1998**, *24*, 55−65.
(28) Wligus, T. A. *Prostaglandins Other Lipid Mediators* **2000**, *62*, 367−84.
(29) Epstein, J. H. *Natl. Cancer Inst. Monogr.* **1978**, *50*, 13−25.
(30) Hildesheim, J.; Fornace, A. J. *DNA Repair (Amst)* **2004**, *3*, 567−80.
(31) Gomez, L. M.; Fernandez, G. L. M.; Jordan, J. *J. Physiol. Biochem.* **2004**, *60*, 287−307.
(32) Tron, V. A.; Li, G.; Ho, V.; Trotter, M. J. *J. Cutan. Med. Surg.* **1999**, *3*, 280−283.
(33) Gough, M.; Hancock, R. E. W.; Kelly N. M. *Infect. Immun.* **1996**, *64*, 4922−4927.
(34) Rabinovich, M. L.; Melnick, M. S.; Bolobova, A. V. *Biochemistry (Mosc)* **2002**, *67*, 850−71.
(35) Kumar, M. U.S. Patent Application 20050142094, 2005.
(36) Holmes, T. C. *Trends Biotechnol.* **2002**, *20*, 16−21.
(37) Chilkoti, A.; Dreher, M. R.; Meyer, D. E. *Adv. Drug Delivery Rev.* **2002**, *54*, 1093−1111.
(38) Bellomo, E. G.; Wyrsta, M. D.; Pakstis, L.; Pochan, D. J.; Deming, T. J. *Nat. Mater.* **2004**, *3*, 244−248.
(39) Silva, G. A.; Czeisler, C.; Niece, K. L.; Beniash, E.; Harrington, D. A. *Science* **2004**, *303*, 1352−13555.
(40) Martin, S. M.; Schwartz, J. L.; Giachelli, C. M.; Ratner, B. D. *J. Biomed. Mater. Res. A* **2004**, *70*, 10−19.
(41) Tosatti, S.; De Paul, S. M.; Askendal, A.; VandeVondele, S.; Hubbell, J. A.; et al. *Biomaterials* **2003**, *24*, 4949−4958.
(42) Sanford, K.; Kumar, M. *Curr. Opin. Biotechnol.* **2005**, *16*, 416−421.

BM060464A